Dependence of above-threshold ionization spectrum on polarization directions of two-color laser fields*

Liu Min(刘 敏)[a)b)], Guo Ying-Chun(郭迎春)[a)†], and Wang Bing-Bing(王兵兵)[b)‡]

[a)] *Department of Physics, East China Normal University, Shanghai* 200241, *China*
[b)] *Laboratory of Optical Physics, Beijing National Laboratory for Condensed Matter Physics, Institute of Physics, Chinese Academy of Sciences, Beijing* 100190, *China*

(Received 23 December 2014; revised manuscript received 5 March 2015; published online 18 May 2015)

Using the frequency-domain theory, we investigate the above-threshold ionization (ATI) process of an atom in two-color laser fields. When both photon energies of the two-color laser fields are much smaller than the atomic ionization threshold, the ATI spectrum depends on the angle between the two lasers' polarization directions. While when the photon energy of one laser is comparable with or larger than the atomic ionization threshold, the ATI spectrum is independent of the angle, and only several dips appear at certain angles. By analyzing the contributions of different quantum channels, we find that, for the case that both frequencies of the two color lasers are low, the quantum interferences between the channels are strong, and hence the spectrum changes with the angle between the two lasers' polarization directions. While for the case that the frequency of one of the two color lasers is high, the contributions of the channels to the ATI spectrum decrease dramatically with increasing channel order, hence the interferences between the channels disappear, and the ATI spectrum has a step-like structure, which is independent of the angle between the two lasers' polarizations. These results can shed light on the study of the corresponding relation between classical and quantum mechanisms of the matter–laser interaction in high-frequency laser fields.

Keywords: above-threshold ionization, two-color laser fields, quantum interference

PACS: 32.80.Rm, 42.50.Hz, 42.65.Ky **DOI:** 10.1088/1674-1056/24/7/073201

1. Introduction

The interaction between an atom and an intense laser pulse can cause lots of fundamental strong-field physics phenomena, such as above-threshold ionization (ATI), high-harmonic generation (HHG), and nonsequential double ionization (NSDI). In the above-threshold ionization, atoms or molecules absorb more photons than necessary for ionization, which was firstly discovered by Agostini *et al.*[1] Since the discovery of ATI, the ionization of an atom in two-color laser pulses has attracted much attention for understanding the stimulated absorption and emission of photons in the ATI process.[2–7] Muller *et al.* observed a sideband structure in the ATI spectrum, which may be due to the stimulated absorption and emission of low-frequency photons.[2] Koval *et al.* investigated the ATI process of an atom in a two-color laser field of the first and the third harmonics. They found that the cutoff of the ATI spectrum depends on the relative phase between the two color laser fields.[7] Furthermore, Paulus *et al.* also found that the cutoff of the photoelectron spectrum strongly depends on the relative phase of the two color laser fields with the frequencies being the fundamental and the second harmonics.[5]

Recently, with the development of high-frequency attosecond pulse techniques via HHG and free-electron lasers, ionization of atoms in IR+XUV two-color laser fields has become a hot topic.[8–18] Kazansky *et al.* investigated the angle-resolved spectra of photoelectrons produced by IR+XUV two-color laser pulses. Radcliffe *et al.* observed a plateau-shape envelope of the ATI spectrum with increasing intensity of the IR laser field. Moreover, Zhang *et al.* found a step-like structure of the ATI spectrum in IR+XUV two-color laser fields. In this paper, we investigate the dependence of the ATI spectrum on the polarization directions of the two-color laser fields. We find that, when the photon energies of both lasers are much smaller than the atomic ionization threshold, the ionization channel interference is very obvious, and hence the ionization spectrum strongly depends on the angle between the two lasers' polarization directions. While when one laser's photon energy approaches or is larger than the atomic ionization threshold, the channel interference disappears, hence the ATI spectrum is independent of the angle between the two lasers' polarization directions, and several dips appear in the spectrum at certain angles.

2. Theoretical method

The frequency-domain theory for the ATI process of an atom in a two-color laser field has been presented in detail.[18–20] Here we briefly summarize the basic idea of this theory for completeness and modify the theory for the case in

*Project supported by the National Natural Science Foundation of China (Grant Nos. 11474348 and 61275128).
†Corresponding author. E-mail: ycguo@phy.ecnu.edu.cn
‡Corresponding author. E-mail: wbb@aphy.iphy.ac.cn
© 2015 Chinese Physical Society and IOP Publishing Ltd

which the two linear polarized lasers have different polarization directions. Atomic units are used throughout the paper, unless specified otherwise. We consider the ionization of an atom in a two-color laser field. The Hamiltonian of this atom–laser system is $H = H_0 + U(r) + V$, where

$$H_0 = \frac{(-\mathrm{i}\nabla)^2}{2} + \omega_1 N_1 + \omega_2 N_2 \tag{1}$$

is the free-electron and free-photon Hamiltonian, N_i is the photon number operator of the field with frequency ω_i, $i = 1,2$, $U(r)$ is the atomic binding potential, and V describes the electron–photon interaction. Based on the formal scattering theory of multiphoton ionization in strong fields,[21] the transition matrix from the initial quantum state ψ_i to the final state ψ_f can be expressed as

$$T_\mathrm{fi} = \langle \psi_\mathrm{f} | V | \psi_\mathrm{i} \rangle . \tag{2}$$

The initial quantum state ψ_i can be expressed as

$$|\psi_\mathrm{i}\rangle = \Phi_\mathrm{i}(\boldsymbol{r}) \otimes |n_1\rangle \otimes |n_2\rangle , \tag{3}$$

with the initial energy being $E_\mathrm{i} = -I_\mathrm{p} + (n_1 + 1/2)\omega_1 + (n_2 + 1/2)\omega_2$. Here, $\Phi_\mathrm{i}(\boldsymbol{r})$ is the ground state of the atom, $|n_j\rangle$ is the Fock state with photon number n_j $(j = 1,2)$, and I_p is the ionization threshold of the atom. The final state ψ_f, which is the quantized-field Volkov state, can be represented as[19,20]

$$\begin{aligned} |\Psi_{\boldsymbol{p}_\mathrm{f},m_1,m_2}\rangle \;=\; & V_\mathrm{e}^{-1/2} \exp\left[\mathrm{i}\left(\boldsymbol{p}_\mathrm{f} + u_{p_1}\boldsymbol{k}_1 + u_{p_2}\boldsymbol{k}_2\right)\cdot\boldsymbol{r}\right] \\ & \times \sum_{j_1=-m_1, j_2=-m_2}^{\infty} \mathcal{J}_{j_1 j_2}(z)^* \\ & \times \exp\left\{-\mathrm{i}\left[j_1\left(\boldsymbol{k}_1\cdot\boldsymbol{r} + \phi_1\right) + j_2\left(\boldsymbol{k}_2\cdot\boldsymbol{r} + \phi_2\right)\right]\right\} \\ & \times |m_1 + j_1, m_2 + j_2\rangle, \end{aligned} \tag{4}$$

where V_e is the normalization volume, $\boldsymbol{p}_\mathrm{f}$ is the momentum of the ionized electron, u_{p_j} is the ponderomotive energy in units of frequency ω_j, and $\boldsymbol{k}_j$ is the photon momentum of the two laser fields with $j = 1,2$. The ϕ_j is the initial phase of the two laser fields, which is set to be zero for simplicity in this paper. The total energy of the final state is

$$E_{\boldsymbol{p}_\mathrm{f},m_1,m_2} = \frac{\boldsymbol{p}_\mathrm{f}^2}{2} + \left(m_1 + \frac{1}{2}\right)\omega_1 + \left(m_2 + \frac{1}{2}\right)\omega_2, \tag{5}$$

where m_1 and m_2 are the photon numbers in the two laser fields.

In Eq. (4), the generalized Bessel function can be written as

$$\begin{aligned} & \mathcal{J}_{j_1,j_2}(z) \\ = & \sum_{q_3 q_4 q_5 q_6} J_{-j_1+2q_3+q_5+q_6}(z_1) J_{-j_2+2q_4+q_5-q_6}(z_2) J_{-q_3}(z_3) \\ & \times J_{-q_4}(z_4) J_{-q_5}(z_5) J_{-q_6}(z_6). \end{aligned} \tag{6}$$

Here, $\boldsymbol{z} \equiv (z_1, z_2, z_3, z_4, z_5, z_6)$, and we have

$$\begin{aligned} & z_1 = -2\sqrt{\frac{u_{p1}}{\omega_1}}\boldsymbol{p}_\mathrm{f}\cdot\boldsymbol{\epsilon}_1, \quad z_2 = -2\sqrt{\frac{u_{p2}}{\omega_2}}\boldsymbol{p}_\mathrm{f}\cdot\boldsymbol{\epsilon}_2, \\ & z_3 = \frac{1}{2}\boldsymbol{\epsilon}_1\cdot\boldsymbol{\epsilon}_1 u_{p_1}, \quad z_4 = \frac{1}{2}\boldsymbol{\epsilon}_2\cdot\boldsymbol{\epsilon}_2 u_{p2}, \\ & z_5 = 2\frac{\sqrt{u_{p1}\omega_1 u_{p2}\omega_2}}{\omega_1 + \omega_2}\boldsymbol{\epsilon}_1\cdot\boldsymbol{\epsilon}_2, \\ & z_6 = 2\frac{\sqrt{u_{p1}\omega_1 u_{p2}\omega_2}}{\omega_1 - \omega_2}\boldsymbol{\epsilon}_1{}^*\cdot\boldsymbol{\epsilon}_2, \end{aligned} \tag{7}$$

where $\boldsymbol{\epsilon}_1$ and $\boldsymbol{\epsilon}_2$ are the polarization directions of the two laser fields. By using the initial and the final states, equation (2) can be expressed as

$$T_\mathrm{d}^s = \sum_{s_2} T_{s_2}, \tag{8}$$

with

$$T_{s_2} = (u_{p1}\omega_1 + u_{p2}\omega_2 - s\omega_1)\Phi_\mathrm{i}(\boldsymbol{p}_\mathrm{f}) J_{s_1,s_2}(\varsigma), \tag{9}$$

where $s\omega_1 = s_1\omega_1 + s_2\omega_2$ is the total photon energy that the electron absorbs from both laser fields, and $s_1 = n_1 - m_1$ and $s_2 = n_2 - m_2$ are the absorbed photon numbers from the two laser fields. We now define θ_1 (θ_2) as the angle between the polarized direction of the first (second) laser field and the emission direction of the ionized electron, θ_3 as the angle between the polarized directions of the two laser fields, then the generalized Bessel function in Eq. (6) can be rewritten as

$$\begin{aligned} & \mathcal{J}_{s_1,s_2}(\varsigma) \\ = & \sum_{q_3 q_4 q_5 q_6} J_{-s_1+2q_3+q_5+q_6}(\varsigma_1) J_{-s_2+2q_4+q_5-q_6}(\varsigma_2) J_{-q_3}(\varsigma_3) \\ & \times J_{-q_4}(\varsigma_4) J_{-q_5}(\varsigma_5) J_{-q_6}(\varsigma_6), \end{aligned} \tag{10}$$

where

$$\begin{aligned} & \varsigma_1 = -2\sqrt{\frac{u_{p1}}{\omega_1}}|\boldsymbol{p}_\mathrm{f}|\cos\theta_1, \\ & \varsigma_2 = -2\sqrt{\frac{u_{p2}}{\omega_2}}|\boldsymbol{p}_\mathrm{f}|\cos\theta_2, \\ & \varsigma_3 = \frac{1}{2}u_{p1}, \quad \varsigma_4 = \frac{1}{2}u_{p2}, \\ & \varsigma_5 = 2\frac{\sqrt{u_{p1}\omega_1 u_{p2}\omega_2}}{\omega_1 + \omega_2}\cos\theta_3, \\ & \varsigma_6 = 2\frac{\sqrt{u_{p1}\omega_1 u_{p2}\omega_2}}{\omega_1 - \omega_2}\cos\theta_3, \end{aligned} \tag{11}$$

with c being the speed of light. In this paper, the emission direction of the ionized electron is set along the first laser's polarization direction, hence we have $\theta_1 = 0$, and assume $\theta_2 = \theta_3 = \theta$.

3. ATI spectrum versus the polarization directions of the two-color lasers

Figure 1 presents the photoelectron spectra as a function of the angle θ between the polarization directions of the two lasers with $\omega_2 = 2\omega_1$, $4\omega_1$, $6\omega_1$, $8\omega_1$, $10\omega_1$, and $30\omega_1$. The

frequency of the first laser is $\omega_1 = 1.165$ eV. The laser intensity $I_1 = I_2 = 3.6 \times 10^{13}$ W/cm^2, corresponding to the ponderomotive value of the first laser $U_{p1} = 3.2\omega_1$, and that of the second laser $U_{p2} = 0.8\omega_1$, $0.20\omega_1$, $0.089\omega_1$, $0.05\omega_1$, $0.032\omega_1$, and $0.0036\omega_1$ for $\omega_2 = 2\omega_1$, $4\omega_1$, $6\omega_1$, $8\omega_1$, $10\omega_1$, and $30\omega_1$, respectively. The ionization threshold of the hydrogen-like atom is $I_p = 12.1$ eV. One can find that the spectrum strongly depends on the angle θ for the case of $\omega_2 = 2\omega_1$, as shown in Fig. 1(a), where the cutoffs for $\theta = 0$ and 180° are about $26\omega_1$ and $10\omega_1$, respectively. As shown in Figs. 1(b)–1(f), when ω_2 increases, the dependence of the spectrum on the angle decreases rapidly, and the spectrum with $\omega_2 = 30\omega_1$ shows a symmetrical structure.

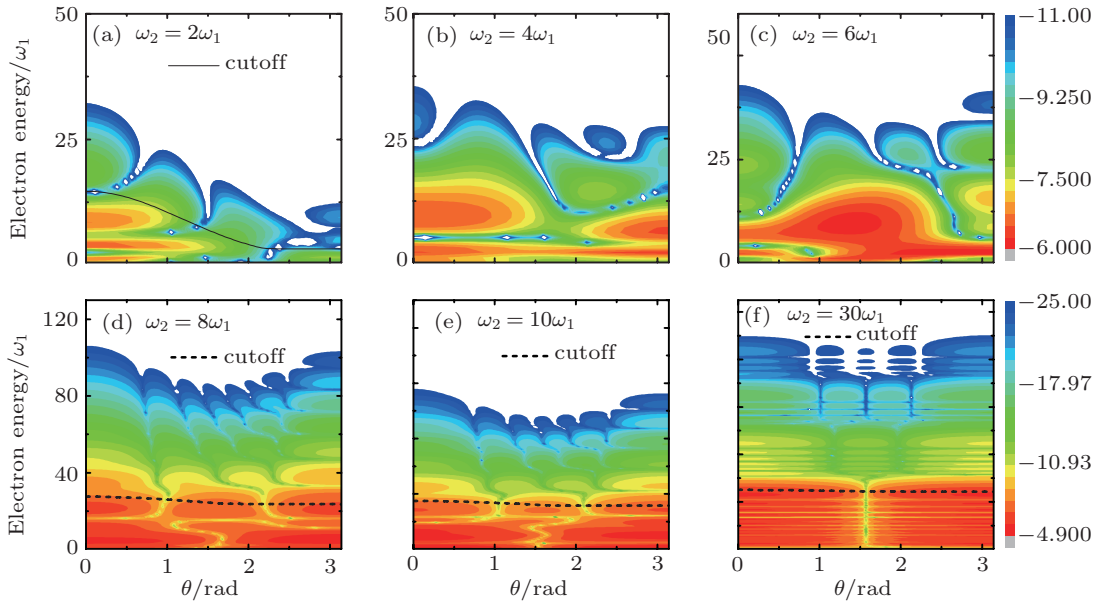


Fig. 1. (color online) Electron spectra as a function of the angle between the two lasers' polarization directions in two-color laser fields with $\omega_1 = 1.165$ eV, and $\omega_2 = 2\omega_1$ (a), $4\omega_1$ (b), $6\omega_1$ (c), $8\omega_1$ (d), $10\omega_1$ (e), $30\omega_1$ (f). The laser intensity $I_1 = I_2 = 3.6 \times 10^{13}$ W/cm^2.

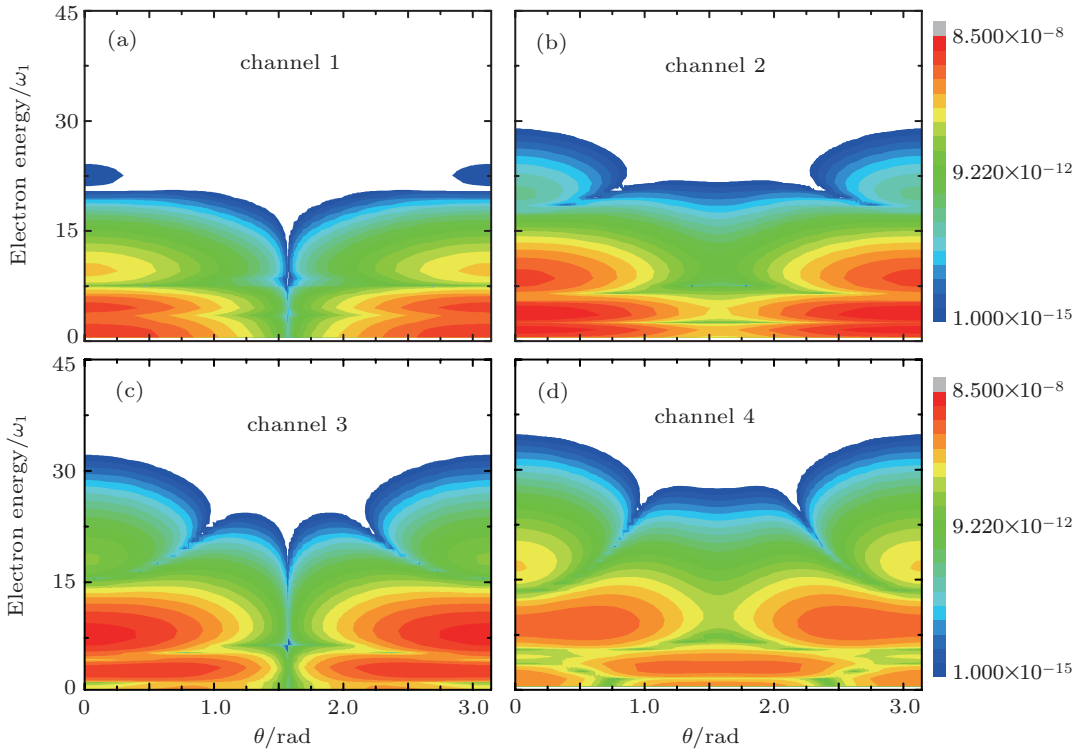


Fig. 2. (color online) ATI spectra as a function of the angle between the two lasers' polarization directions for channel 1 (a), 2 (b), 3 (c), and 4 (d) with $\omega_1 = 1.165$ eV, $\omega_2 = 2\omega_1$. The laser intensity $I_1 = I_2 = 3.6 \times 10^{13}$ W/cm^2.

To understand the spectral characteristics shown in Fig. 1, we define the quantum channel by the photon number s_2 that the atom absorbs from the high-frequency laser. Therefore, the transition matrix of the s_2 channel is expressed by Eq. (9). Figures 2 and 3 present the ATI spectra as a function of angle θ for different channels with $\omega_2 = 2\omega_1$ and $10\omega_1$, respectively. We find that all spectra are symmetrical about $\theta = \pi/2$. However, the cutoff of the spectrum for the case of $\omega_2 = 2\omega_1$ decreases as the angle increases from 0 to $\pi/2$, as shown in Fig. 2; while that for the case of $\omega_2 = 10\omega_1$ keeps unchanged as the angle increases and the spectrum only shows several dips at certain angles for different channels.

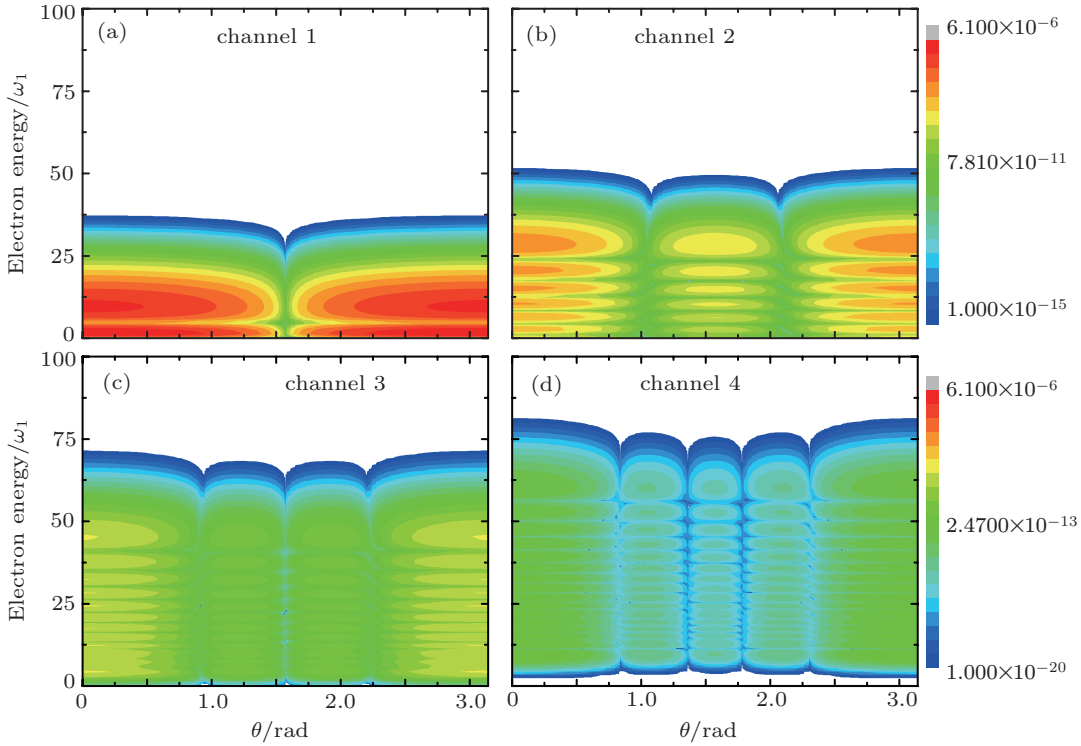


Fig. 3. (color online) ATI spectra as a function of the angle between the two lasers' polarization directions for channel 1 (a), 2 (b), 3 (c), and 4 (d) with $\omega_1 = 1.165$ eV and $\omega_2 = 10\omega_1$. The laser intensity $I_1 = I_2 = 3.6 \times 10^{13}$ W/cm^2.

By analyzing the property of the Bessel function in Eq. (9), the symmetry characteristics of the spectra for all channels shown in Figs. 2 and 3 can be explained as follows. By using the integral formula of the Bessel function

$$J_n(z) = \frac{1}{2\pi}\int_{-\pi}^{\pi} \exp[\mathrm{i}(n\alpha - z\sin\alpha)]\,\mathrm{d}\alpha, \tag{12}$$

we can express the Bessel function by its Taylor's series expansion as

$$J_n(z) = \delta_{n,0} + \frac{1}{2}(\delta_{n,1} - \delta_{n,-1})z + \frac{1}{8}(\delta_{n,2} + \delta_{n,-2} - 2\delta_{n,0})z^2 + \cdots. \tag{13}$$

By inserting the Taylor expansions of Bessel functions $J_{-s_2+2q_4+q_5-q_6}(\varsigma_2)$, $J_{-q_5}(\varsigma_5)$, and $J_{-q_6}(\varsigma_6)$ into Eq. (9), for the odd channels with $s_2 = 2n+1, n = 0, 1, \ldots$, the Bessel function can be rewritten as

$$\mathcal{J}_{s_1,s_2}(\varsigma) = \sum_{n=0}^{\infty} A_n \cos^{2n+1}\theta; \tag{14}$$

while for the even channels with $s_2 = 2n, n = 0, 1, \ldots$, it can be expressed as

$$\mathcal{J}_{s_1,s_2}(\varsigma) = \sum_{n=0}^{\infty} B_n \cos^{2n}\theta. \tag{15}$$

Since the ionization rate Γ of each channel is proportional to $|\mathcal{J}_{s_1,s_2}(\varsigma)|^2$, we therefore find that $\Gamma \propto \sum_{n=0}^{\infty} C_n \cos^{2n+2}\theta$ for the odd channels, and $\Gamma \propto \sum_{n=0}^{\infty} D_n \cos^{2n}\theta$ for the even channels, where C_n and D_n are nonzero parameters which can be obtained by using Eq. (10). As a result, the spectra of all channels are symmetrical about $\theta = \pi/2$.

Comparing the spectra of Figs. 1(a) and 1(f), we find that, for the case of $\omega_2 = 2\omega_1$, the cutoff of the total ATI spectrum decreases as θ increases from 0 to π, and the spectral symmetry for separate channels shown in Fig. 2 completely disappears; while for the case of $\omega_2 = 30\omega_1$, the ATI spectrum shows a multi-plateau structure with the cutoff of each plateau being independent of the angle θ, and the symmetry of the channel spectra about $\theta = \pi/2$ remains. To understand these differences, we present the ATI spectra for the first five

channels with $\theta = 0$, 180° and $\omega_2 = 2\omega_1$, $4\omega_1$, $6\omega_1$, $10\omega_1$ in Fig. 4. We find that the five channels have comparable contributions to the total ATI spectrum when $\omega_2 = 2\omega_1$, as shown in Figs. 4(a) and 4(e). While only the first three channels dominate the contributions to the spectrum when $\omega_2 = 4\omega_1$, as shown in Figs. 4(b) and 4(f). Finally, the contributions to the spectrum from different channels completely separate and the ATI spectrum has a step-like structure when $\omega_2 \geq 10\omega_1$, as shown in Figs. 4(d) and 4(h). The quantum interference of the channels induces the dramatic dependence of the ATI spectrum on the angle θ for the case of $\omega_2 = 2\omega_1$; while the interference between the channels disappears for $\omega_2 \geq 10\omega_1$, and hence the total spectrum is independent of the angle.

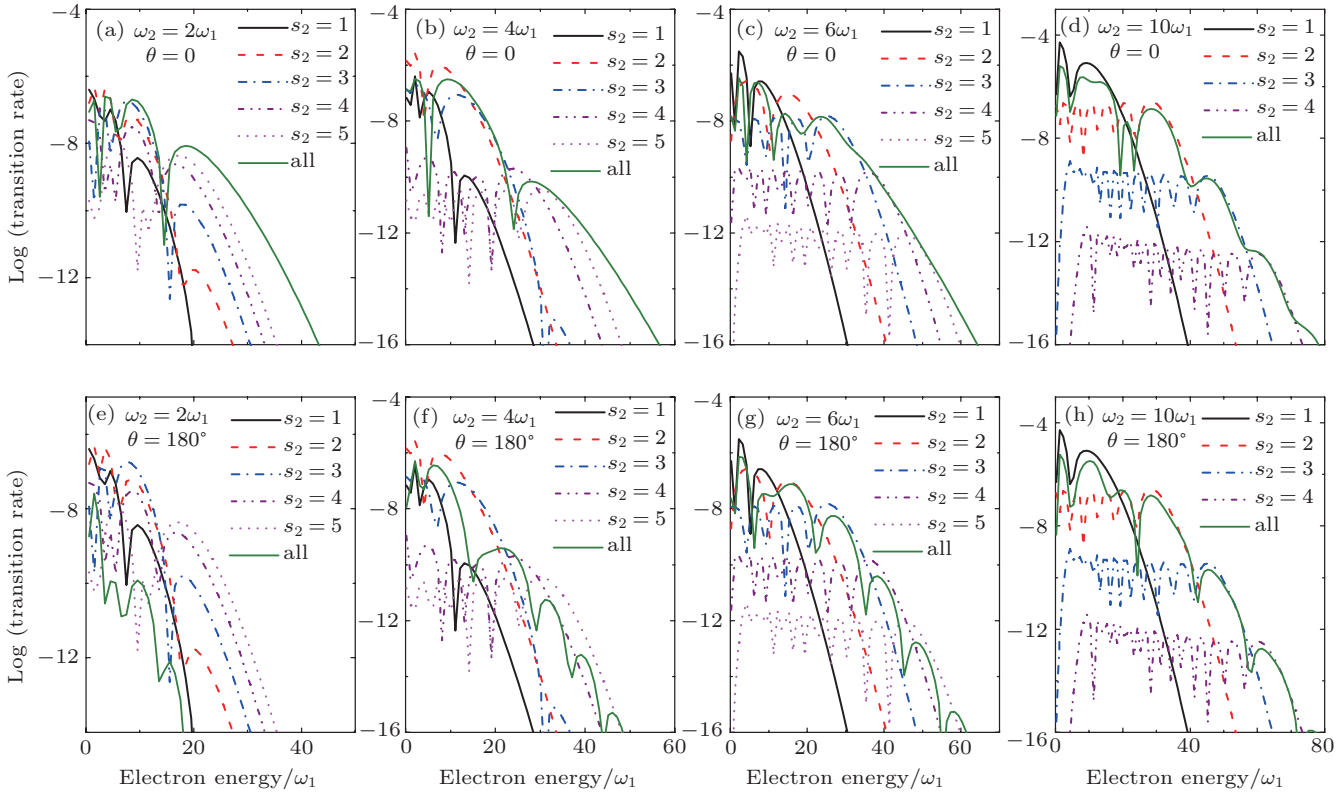


Fig. 4. (color online) Electron spectra for different channels with the angle between the two lasers' polarization directions $\theta = 0$ ((a)–(d)) and 180° ((e)–(h)). Here $\omega_1 = 1.165$ eV, and $\omega_2 = 2\omega_1$ ((a) and (e)), $4\omega_1$ ((b) and (f)), $6\omega_1$ ((c) and (g)), $10\omega_1$ ((d) and (h)).

When $\omega_2 = 2\omega_1$, we may regard both lasers as classical fields, hence we can obtain the cutoff of the total ATI spectrum by using the saddle-point approximation to the Bessel function in Eq. (8).[22–25] In general, the classical action function $S_c(\boldsymbol{p}_f, t) = \frac{1}{2}\int_0^t \mathrm{d}t'[\boldsymbol{p}_f - e\boldsymbol{A}_c(t')]^2$ of an electron moving in a two-color laser field $\boldsymbol{A}_c(t) = \boldsymbol{\epsilon}_1 A_1 \cos(\omega_1 t) + \boldsymbol{\epsilon}_2 A_2 \cos(\omega_2 t)$ can be written as

$$\begin{aligned} S_c(\boldsymbol{p}_f, t) = & \left(\frac{\boldsymbol{p}_f^2}{2} + U_{p1} + U_{p2}\right)t \\ & - z_1 \sin(\omega_1 t) - z_2 \sin(\omega_2 t)\cos\theta + z_3 \sin(2\omega_1 t) \\ & + z_4 \sin(2\omega_2 t) + z_5 \sin[(\omega_1 + \omega_2)t]\cos\theta \\ & + z_6 \sin[(\omega_1 - \omega_2)t]\cos\theta, \end{aligned} \tag{16}$$

where $\boldsymbol{p}_f$ is set along the direction of $\boldsymbol{\epsilon}_1$, and the angle between $\boldsymbol{\epsilon}_1$ and $\boldsymbol{\epsilon}_2$ is θ, which corresponds to the quantum numerical calculation condition. On the other hand, by using the integral form of the Bessel function, the generalized Bessel function Eq. (11) can be written as

$$\begin{aligned} & \mathcal{J}_{s_1,s_2}(z) \\ & = \frac{1}{T^2}\int_{-T/2}^{T/2}\int_{-T/2}^{T/2} \mathrm{d}t_1\,\mathrm{d}t_2 \exp\{\mathrm{i}[-z_1 \sin(\omega_1 t_1) - z_2 \sin(\omega_2 t_2)\cos\theta \\ & + z_3 \sin(2\omega_1 t_1) + z_4 \sin(2\omega_2 t_2) + z_5 \sin(\omega_1 t_1 + \omega_2 t_2)\cos\theta \\ & + z_6 \sin(\omega_1 t_1 - \omega_2 t_2)\cos\theta + s_1\omega_1 t_1 + s_2\omega_2 t_2]\}, \end{aligned} \tag{17}$$

hence we have

$$\begin{aligned} & \sum_{s_2} \mathcal{J}_{s_1,s_2}(z) \\ & = \frac{1}{T}\int_{-T/2}^{T/2} \mathrm{d}t_1 \exp\{\mathrm{i}[-z_1 \sin(\omega_1 t_1) - z_2 \sin(\omega_2 t_1)\cos\theta \\ & + z_3 \sin(2\omega_1 t_1) + z_4 \sin(2\omega_2 t_1) + z_5 \sin[(\omega_1 + \omega_2)t_1]\cos\theta \\ & + z_6 \sin[(\omega_1 - \omega_2)t_1]\cos\theta + (s_1\omega_1 + s_2\omega_2)t_1]\}. \end{aligned} \tag{18}$$

Therefore, we obtain the relationship between the Bessel function and the classical action function

$$\sum_{s_2} J_{s_1,s_2}(z) = \frac{1}{T}\int_{-T/2}^{T/2} \mathrm{d}t_1 \exp\{\mathrm{i}[S_\mathrm{c}(t_1) + I_\mathrm{p} t_1]\}, \tag{19}$$

where $p_\mathrm{f}^2/2 + U_{p1} + U_{p2} + I_\mathrm{p} = s_1\omega_1 + s_2\omega_2$. By using the saddle-point approximation, we obtain the energy equation from Eq. (19)

$$\frac{1}{2}[\boldsymbol{p}_\mathrm{f} - e\boldsymbol{A}_\mathrm{c}(t)]^2 + I_\mathrm{p} = 0, \tag{20}$$

which has the same form as that in the monochromatic low-frequency laser case.[26] By setting I_p to 0, we obtain the cutoff of the ATI spectrum with Eq. (20), which is shown by the solid curve in Fig. 1(a). We find that the cutoff curve agrees well with the quantum numerical results. These results indicate that the ATI spectrum depends on the angle between the two laser polarization directions when both laser fields can be treated as classical fields.

However, when $\omega_2 \geq 10\omega_1$, the high-frequency laser field must be regarded as a quantum field, rather than a classical one. Therefore, the cutoff equation (20) is no longer suitable for the high-frequency laser case. Under our present calculation conditions, we find that the spectra for different channels completely separate from each other, as shown in Figs. 1(d)–1(f), hence the ATI transition matrix element now becomes $T_\mathrm{d}^s = \sum_{s_2} T_{s_2}$. Furthermore, the arguments of ς_4, ς_5, and ς_6 in the Bessel function of Eq. (10) are much smaller than 1 due to the small value of U_{p2} for $\omega_2 \geq 10\omega_1$. Therefore, the Bessel function $J_{qi}(\varsigma_i) \approx 0$ for $i = 4, 5, 6$ in Eq. (10), and hence the Bessel function of Eq. (10) can be simplified as[18]

$$\mathcal{J}_{s_1 s_2}(\zeta) \approx J_{-s_1}(\zeta_1, \zeta_3) J_{-s_2}(\zeta_2), \tag{21}$$

where s_1 and s_2 are the numbers of photons of frequencies ω_1 and ω_2 that the electron absorbs, and $\mathcal{J}_{-s_1}(\zeta_1, \zeta_3) = \sum_{q_3} J_{-s_1+2q_3}(\zeta_1) J_{-q_3}(\zeta_3)$. As a result, the matrix element of channel s_2 can be written as

$$\begin{aligned} T_{s_2} &= (u_{p1}\omega_1 + u_{p2}\omega_2 - s\omega_1) \\ &\quad \times \Phi_\mathrm{i}(\boldsymbol{p}_\mathrm{f}) J_{-s_1}(\zeta_1, \zeta_3) J_{-s_2}(\zeta_2). \end{aligned} \tag{22}$$

Although the high-frequency ω_2 laser field cannot be treated as a classical field, the low-frequency ω_1 laser field can still be regarded as a classical field. Therefore, the cutoff of the ATI spectrum for each s_2 channel can be obtained by using the saddle-point approximation for the Bessel function $J_{-s_1}(\zeta_1, \zeta_3)$ in Eq. (22) with a certain value of s_2. Similarly, we now have the energy relationship

$$\frac{[\boldsymbol{p}_\mathrm{f} - e\boldsymbol{A}_{\mathrm{c}1}(t)]^2}{2} = \left(s_2\omega_2 - I_\mathrm{p}\right). \tag{23}$$

The dashed lines in Figs. 1(d)–1(f) show the cutoff with $s_2 = 1$ obtained by Eq. (23) with I_p keeping its value. We find that the cutoff curves agree well with the numerical calculation. Moreover, since the cutoff formula is independent of the high-frequency ω_2 laser field, the cutoff keeps unchanged with increasing θ.

4. Conclusion

Based on the frequency-domain theory, we investigate the dependence of the ionization of an atom on the angle between the polarization directions of the two laser fields. We find that the angle dependence of the ATI spectrum is related to the frequencies of the two laser fields. When the photon energies of the two lasers are much smaller than the atomic ionization threshold, both laser fields can be regarded as classical fields, hence the channel interferences are very strong, and the ATI spectrum depends on the angle between the two lasers' polarization directions. While when one laser's photon energy is larger than the atomic ionization threshold, this high-frequency laser field can only be treated as a quantum field, and the channel interference disappears, resulting in that the ATI spectrum is independent of the angle between the lasers' polarization directions, and only several dips appear at certain angles.

Acknowledgment

We thank the members of the SFAMP club for their helpful discussions and suggestions.

References

[1] Agostini P, Fabre F, Mainfray G, Petite G and Rahman N K 1979 *Phys. Rev. Lett.* **42** 1127
[2] Muller H, Heuvell H and Wiel M 1986 *J. Phys. B* **19** L733
[3] Ivanov M Yu and Rzazewski K 1992 *J. Mod. Opt.* **39** 2377
[4] Veniard V, Taieb R and Maquet A 1995 *Phys. Rev. Lett.* **74** 4161
[5] Paulus G G, Becker W and Walther H 1995 *Phys. Rev. A* **52** 4043
[6] Han C S 1997 *Phys. Rev. A* **55** 3957
[7] Koval A V and Koval V M 2007 *J. Exp. Theor. Phys.* **104** 210
[8] O'Keeffe P, López-Martens R, Mauritsson J, Johansson A, L'Huillier A, Véniard V, Taïeb R, Maquet A and Meyer M 2004 *Phys. Rev. A* **69** 051401(R)
[9] Meyer M, Cubaynes D, O'Keeffe P, Luna H, Yeates P, Kennedy E T, Costello J T, Orr P, Taïeb R, Maquet A, Düsterer S, Radcliffe P, Redlin H, Azima A, Plönjes E and Feldhaus J 2006 *Phys. Rev. A* **74** 011401(R)
[10] Meyer M, Cubaynes D, Glijer D, Dardis J, Hayden P, Hough P, Richardson V, Kennedy E T, Costello J T, Radcliffe P, Düsterer S, Azima A, Li W B, Redlin H, Feldhaus J, Taïeb R, Maquet A, Grum-Grzhimailo A N, Gryzlova E V and Strakhova S I 2008 *Phys. Rev. Lett.* **101** 193002
[11] Meyer M, Costello J T, Düsterer S, Li W B and Radcliffe P 2010 *J. Phys. B* **43** 194006
[12] Radcliffe P, Arbeiter M, Li W B, Düsterer S, Redlin H, Hayden P, Hough P, Richardson V, Costello J T, Fennel T and Meyer M 2012 *New J. Phys.* **14** 043008
[13] Radcliffe P, Arbeiter M, Li W B, Düsterer S, Redlin H, Hayden P, Hough P, Richardson V, Costello J T, Fennel T and Meyer M 2012 *New J. Phys.* **14** 043008
[14] Kazansky A K, Sazhina I P and Kabachnik N M 2010 *Phys. Rev. A* **82** 033420

[15] Kazansky A K, Sazhina I P and Kabachnik N M 2012 *Phys. Rev. A* **86** 033404
[16] Kazansky A K, Sazhina I P and Kabachnik N M 2013 *J. Phys. B* **46** 025601
[17] Shivaram N, Timmers H, Tong X M and Sandhu A 2013 *Chem. Phys.* **414** 139
[18] Zhang K, Chen J, Hao X L, Fu P, Yan Z C and Wang B 2013 *Phys. Rev. A* **88** 043435
[19] Guo D S and Drake G 1992 *J. Phys. A* **25** 5377
[20] Gao L, Li X, Fu P and Guo D S 1998 *Phys. Rev. A* **61** 3807
[21] Guo D S, Aberg T and Crasemann B 1989 *Phys. Rev. A* **40** 4997
[22] Wang B, Gao L, Li X, Guo D and Fu P 2007 *Phys. Rev. A* **75** 063419
[23] Guo Y, Fu P, Yan Z, Gong J and Wang B 2009 *Phys. Rev. A* **80** 063408
[24] Wang B, Guo Y, B. Zhang, Zhao Z, Yan Z C and Fu P 2010 *Phys. Rev. A* **82** 043402
[25] Wang B, Guo Y, Chen J, Yan Z C and Fu P 2012 *Phys. Rev. A* **85** 023402
[26] Lewenstein M, Balcou P, Ivanov M, L'Huillier A and Corkum P B 1994 *Phys. Rev. A* **49** 2117